

Optical Design and Analysis of a Novel Spectral Beam Splitting Hybrid Photovoltaic and Concentrating Solar Thermal System

Xin Zhang^{1,2,3,4}, Dongqiang Lei^{1,2,3,4}, Bo Zhang⁵, Zhifeng Wang^{1,2,3,4}

¹ Key Laboratory of Concentrating solar thermal Energy and Photovoltaic System, Chinese Academy of Sciences, Beijing (China)

² Institute of Electrical Engineering, Chinese Academy of Sciences, Beijing (China)

³ University of Chinese Academy of Sciences, Beijing (China)

⁴ Beijing Engineering Research Center of Concentrating solar thermal Power, Beijing (China)

⁵ North University of China, Taiyuan, Shanxi (China)

Abstract

A simple and compact photovoltaic and concentrating solar thermal (PV/CST) hybrid system with a spectral beam splitting film is proposed in this study. The novel spectral beam splitting film is laid on a PV cell, which exhibits a superior spectral beam splitting, simultaneously achieving high average transmittance of 86.26% and reflectance of 54.03%. The Monte Carlo Ray-Trace Method (MCRT) is used to simulate the path of light and the concentrating characteristic between the primary reflect mirrors and absorber tube of the PV/CST hybrid system. The solar energy flux distribution on the surface of outer wall of the absorber tube is calculated via utilizing MCRT method. The photoelectric and photothermal characteristics of the PV and photothermal sub-unit are studied with and without ITO SBS filter, respectively. The total energy of hybrid PV/CST system using ITO SBS filters was greater than a single PV unit by 33.3%, but decreased by 5.69% compared to individual photothermal units, with this system demonstrating considerable potential for application.

Keywords: Photovoltaic, concentrating solar thermal, spectral beam splitting film, solar energy flux distribution, Monte Carlo Ray-Trace Method

1. Introduction

Energy crisis is a global problem, owing to the increase in energy demand. In the current era, the depletion of traditional fossil energy and the severe environmental problems have promoted the vigorous development of renewable energy. Among them, clean, abundant and flexible solar energy has been vigorously promoted and applied by various countries (Zhou et al., 2020) Solar thermal and photovoltaic (PV) as chief technologies in the application of solar energy utilization. However, solar thermal utilization covers a large area and has low photothermal efficiency (Felsberger et al., 2021). The PV utilization has strong spectral selection properties (Cao et al., 2016). For meeting the requirement of maximized utilized solar energy, the photovoltaic and concentrating solar thermal (PV/CST) hybrid system with a spectral beam splitting (SBS) filter was proposed. The films achieve superior spectral beam splitting, which can transmit the wavelengths of sunlight that effectively produce electricity to the PV cells, but the unwanted wavelengths of sunlight for PV to the solar receiver for thermal energy (Zhang et al., 2021).

Most of the SBS filters mentioned in the above studies, including solid interference filter (Wang et al., 2020), liquid absorptive filter (Han et al., 2020), holographic filter (Ludman et al., 1992), luminescent filter (V and A, 2009), and spectrally selective solar cells (Widyolar et al., 2018), are frequently applied in hybrid PV/CST systems (Zhang et al., 2020). The Monte Carlo Ray-Trace Method (MCRT) as a statistical method of ray tracing, a large number of beams with radiation energy, after tracking the path of the beam, to achieve multiple lights stochastic processes such as reflection, transmission and absorption, statistically obtain the energy flow density distribution of the absorption surface (Qiu et al., 2015). MCRT method are widely used in solar thermal power systems to obtain the energy flow density distribution of the collector (Zhao et al., 2015). For instance, parabolic

trough collector (Cheng et al., 2012), linear Fresnel collector (Ma et al., 2017), dish collector (Hiba et al., 2019), and tower collector (Walzel et al., 1977), etc. However there are few reports on solar energy flux distribution in hybrid PV/CST system with SBS films by adopting MCRT method.

In this paper, the optical model of the PV/CST hybrid system was established in a TracePro software, including PV cells, the SBS filters, and absorber tube. Three-dimensional physical model of the PV cells with the SBS filters are designed to resemble the primary mirror field of the linear Fresnel reflector concentrator. The MCRT simulates the light concentrating characteristics of the absorber tube, and the energy flux distribution of the absorber tube are obtained. Simultaneously, analyzing the concentrating characteristic with and without ITO SBS filters in the PV/CST hybrid system.

2. Physical model

2.1. Optical filter

The optical filters exhibited prominent SBS characteristics with a high average transmittance in the wavelength range of 380–1100 nm and reflectance in the wavelength ranges of 300–380 and 1100–2500 nm, respectively. For improving the experiment efficiency, the simulation was employed to optimize deposition parameters. The design of the optical filter is carried out by using the TFCalc software, which based on the Needle optimization method (Tikhonravov et al., 1996). Considering the outstanding SBS effect and the simple production process, the ITO film was chosen and designed as SBS film. Fig. 1(a) illustrates the transmittance and reflectance spectral with different thickness of ITO films in TFCalc software. It can be seen that with the thickness increased, the transmittance curve moves toward the smaller value and the curve shape changes. Moreover, the whole reflectance spectral moves toward the long wavelength direction and the greater value. However, the actual experimental details can not be obtained through simulations.

The optical filters were prepared on low-iron glass by magnetron sputtering, which were put PV cells. The substrate of low-iron glass has the selective transmittance of light, making the transmittance of middle-infrared (MIR) and infrared (IR) regions of the solar spectrum is low and the visible and near-infrared (NIR) regions is contrary, thus realizing the initial SBS of the infrared spectrum range. The available energy of 380–1100 nm of the solar spectrum in total solar radiation energy is about 65%; the rest of 250–380 nm and 1100–2500 nm is not more than 15% and 20%, respectively. PV systems have strong spectrum selection characteristics, which generates electricity in the wavelength range of 400–1100 nm. The photoelectric characteristics of Si solar cells are observed with the external quantum efficiency (EQE), which indicates the response at wavelengths of 400 to 1100 nm, as illustrated in Fig. 1(b). The EQE of Si solar cell is equal to the ratio of the number of the wavelength-dependent photogenerated carriers or holes contributing to photocurrent to that of incident photons, which can reflect the real photoelectric conversion (PEC) capability of Si solar cell.

Therefore, the solar radiant energy of visible and NIR regions is the focus of our subsequent research. The optical SBS filters of ITO were prepared on glass by magnetron sputtering, which exhibits superior optical performance. The reflectance (ρ) and transmittance (τ) were measured using a Cary 7000 UV/Vis/NIR spectrophotometer. The ITO SBS film is expected to broaden the applications of PV/CST hybrid systems.

The reflectance (ρ) and transmittance (τ) were measured, by Eqs. (1) and (2).

$$\rho = \frac{\int_{0.3 \mu\text{m}}^{0.38 \mu\text{m}} \rho(\theta, \lambda) I_s(\lambda) d\lambda + \int_{1.1 \mu\text{m}}^{2.5 \mu\text{m}} \rho(\theta, \lambda) I_s(\lambda) d\lambda}{\int_{0.3 \mu\text{m}}^{0.38 \mu\text{m}} I_s(\lambda) d\lambda + \int_{1.1 \mu\text{m}}^{2.5 \mu\text{m}} I_s(\lambda) d\lambda} \quad (\text{eq. 1})$$

$$\tau = \frac{\int_{0.38 \mu\text{m}}^{1.1 \mu\text{m}} \tau(\theta, \lambda) I_s(\lambda) d\lambda}{\int_{0.3 \mu\text{m}}^{1.1 \mu\text{m}} I_s(\lambda) d\lambda} \quad (\text{eq. 2})$$

where λ , $\rho(\theta, \lambda)$, $\tau(\theta, \lambda)$, $I_s(\lambda)$ are the wavelength, reflectance at a certain wavelength, transmittance at a certain wavelength, and direct normal solar irradiance, respectively, as defined according to ISO standard 9845-1, normal radiance, air mass 1.5. The ρ and τ are equally weighted fractions.

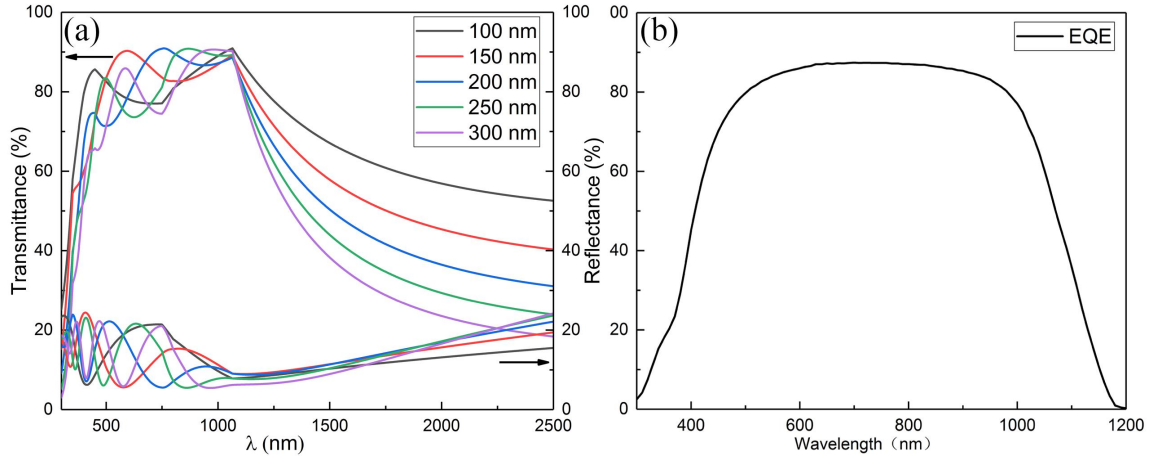


Fig. 1 (a) The simulated spectrum of the different thickness ITO optical filter, (b) the EQE spectra of Si solar cell

2.2. CPC model

The photovoltaic and concentrating solar thermal hybrid system has been designed to use secondary concentrator to increase the energy flux density and make the energy flux distribution uniformly distributed on the receiver tube surface, avoiding generating local flux spots and thus increasing the optical efficiency. The compound parabolic concentrator (CPC) is crucial for the development of hybrid PV/CST systems. As a mature solar heat gathering device, CPC is very popular in concentrating solar systems.

The CPC is a non-imaging concentrator and without tracking of the sun, which includes an involute segment and parabola segment, the curves of the CPC is illustrated in Fig. 2. The theoretical model of CPC was designed by adjusting half-acceptance angle θ_{max} , absorber tube of radius r_1 , and glass tube of radius r_2 . The coordinates of the CPC curve are given by Eq. (3). The CPC collector is designed, which achieves the ray coming into the CPC aperture at an angle smaller than θ_{max} reaches the receiver; otherwise, the ray will return.

$$\begin{cases} x = r_1 \sin\theta - \rho \cos\theta \\ y = -r_1 \cos\theta - \rho \sin\theta \end{cases} \quad (\text{eq. 3})$$

where

$$\rho = r_1(\theta + \beta) \quad \text{for } \arccos(r_1/r_2) \leq \theta \leq \pi/2 + \theta_{max}$$

and

$$\rho = \frac{r_1[\theta + \theta_{max} + \pi/2 + 2\beta - \cos(\theta - \theta_{max})]}{1 + \sin(\theta - \theta_{max})} \quad \text{for } \pi/2 + \theta_{max} \leq \theta \leq 3\pi/2 - \theta_{max}$$

$$\text{then } \beta = \sqrt{(r_2/r_1)^2 - 1} - \arccos(r_1/r_2)$$

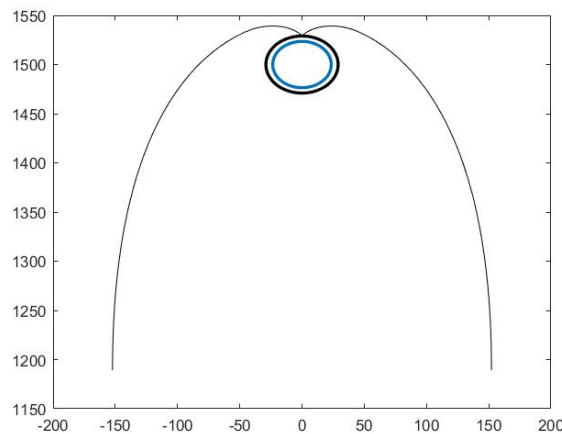


Fig. 2 schematic of CPC

Meanwhile, the design of gap losses and truncation ratio of the CPC will be discussed. The glass tube exists a vacuum environment, which can reduce the heat losses by reducing heat conduction and convection. The gap between the absorber and the CPC reflector is required. However, the gap reduces the rays arrived to CPC and increases the reflection loss of the sun light. The complete CPC has a large reflection plate, but the concentration effect of upper reflection plate is poor. Therefore, an appropriate truncation ratio can reduce material of the reflector.

2.3. System optical model

The linear Fresnel reflector system is an essential precondition for the energy analysis, performance optimization, structure optimization, and operation control of hybrid PV/CST systems. Therefore, the hybrid PV/CST system utilizing SBS filter is improved base on the linear Fresnel reflector system, which consists of a primary mirror field (solar cell and SBS film), a CPC secondary concentrator, and an absorber tube, the schematic diagram of the hybrid PV/CST is shown in Fig. 3. The primary reflector of a tandem structure with an optical filter putting on PV cell, which is supported by a structure made of mild steel or aluminum. The solar radiation is distinguished by SBS film, selecting the solar spectrum regions with high photoelectric conversion rate (in the wavelength range of 400–1100 nm), and transmitting to the surface of the battery for photovoltaic utilization; the rest of the solar radiation is reflected to the absorber tube for photothermal usage (in the wavelength range of 1100–2500 nm).

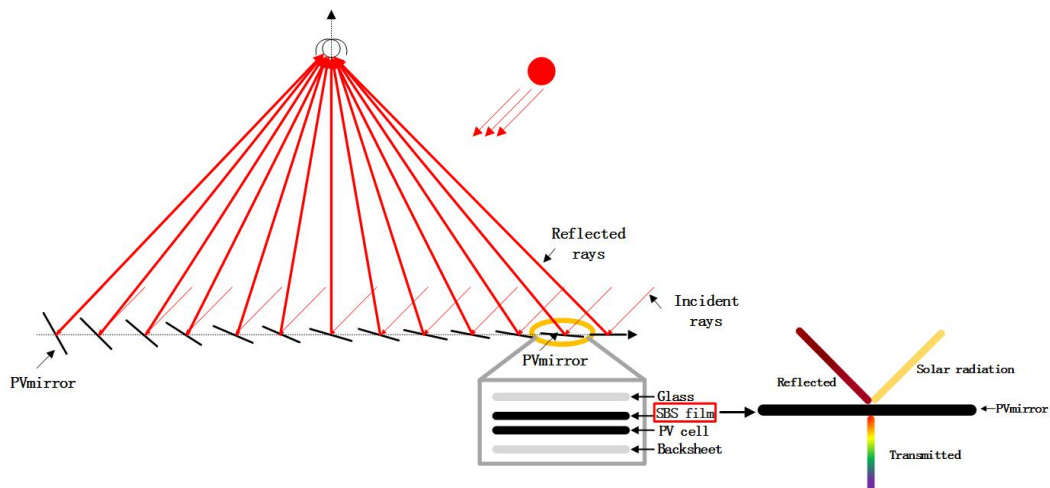


Fig. 3 Hybrid PV/CST system diagram based on the spectral beam splitting film

The geometrical structure of primary mirror field is designed using Tracepro software and Matlab software, which is based on the MCRT Method. Fig. 4 shows the diagram of the Geometrical model of the hybrid PV/CST system, including PV cells, the SBS films, CPC, and absorber tube. The SBS film and CPC still needs to be continuously designed and optimized. The optical parameters of the primary reflectors and absorber tube are listed in Table 1.

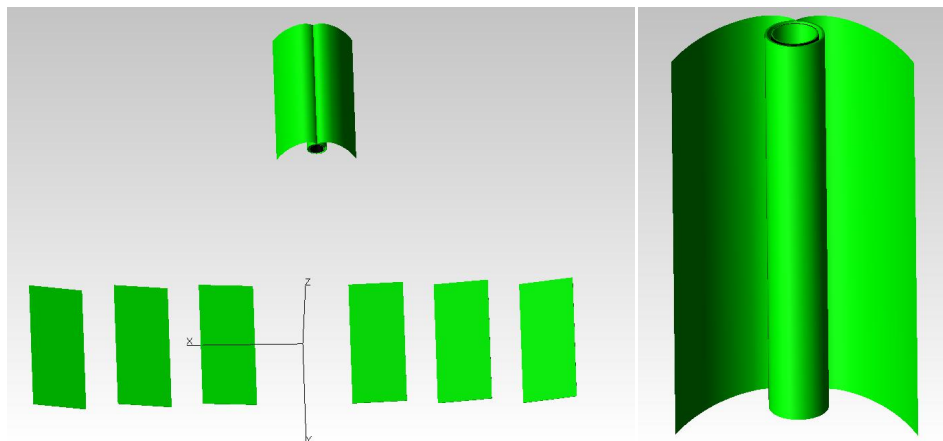


Fig. 4: Geometrical model of the PV/CST hybrid system

Tab. 1: Optical parameters of the PV/CST hybrid system

Component	Item	Value
Single PV cell	width	160 mm
	length	400 mm
	interval	90 mm
Absorber tube	diameter	23.5 mm
	length	400 mm
	thickness	2 mm
	focus	1500 mm
Glass tube	absorbance	0.95
	diameter	29 mm
	length	400 mm
	thickness	3 mm
	transmittance	0.95

After a simple analysis of original and additional ITO SBS film PV Cells by the I-V curve, the energy of the hybrid PV/CST system were theoretically analyzed from the perspective of the law of conservation of energy. The energy obtained by PV cells (E_{PV}) and absorber tube (E_{absorber}) without SBS filters can be calculated by Eqs. (5) and (6):

$$E_{PV} = \int_{0.3 \mu\text{m}}^{1.1 \mu\text{m}} \tau(\theta, \lambda) I_s(\lambda) d\lambda \quad (\text{eq. 5})$$

$$E_{\text{absorber}} = \int_{0.3 \mu\text{m}}^{2.5 \mu\text{m}} \rho(\theta, \lambda)_{\text{mirror}} \alpha(\theta, \lambda) I_s(\lambda) d\lambda \quad (\text{eq. 6})$$

where $\rho(\theta, \lambda)_{\text{mirror}}$ and $\alpha(\theta, \lambda)$ are the reflectance of the primary reflect mirrors at a certain wavelength and absorbance of the absorber tube at a certain wavelength.

The energy obtained by PV cells (E_{PV}) and absorber tube (E_{absorber}) with a 135 nm-thick ITO SBS filters can be calculated by Eqs. (7) and (8):

$$E_{PV, \text{SBS}} = \int_{0.3 \mu\text{m}}^{1.1 \mu\text{m}} \tau(\theta, \lambda)_{\text{SBS}} I_s(\lambda) d\lambda \quad (\text{eq. 7})$$

$$E_{\text{absorber, SBS}} = \int_{1.1 \mu\text{m}}^{2.5 \mu\text{m}} \rho(\theta, \lambda)_{\text{SBS}} \alpha(\theta, \lambda) I_s(\lambda) d\lambda \quad (\text{eq. 8})$$

where $\tau(\theta, \lambda)_{\text{SBS}}$ and $\rho(\theta, \lambda)_{\text{SBS}}$ are the transmittance and reflectance of the ITO SBS filter at a certain wavelength; $\alpha(\theta, \lambda)_{\text{SBS}}$ is the absorbance of the absorber tube at a certain wavelength.

3. Results and discussion

3.1. Optical filter

The SBS performance of the ITO SBS film is shown in Fig. 5(a), which has superior spectral beam splitting. From the figure, the spectrums vary with the thickness of the ITO SBS film. After simulations of the TFCalc software, we selected two samples with a thickness of 135 nm and 185 nm for subsequent experiments, indicated by the red curve and the black curve in Fig. 5(a), respectively. From the figure, we can see that the ITO SBS film are more selective than the glass for the transmitted and reflected spectra. It is clear that increasing the thickness of the ITO SBS film increases the reflectance in the wavelength range of 1100–2500 nm and reduces the transmittance in full spectral wavelength range. The ITO SBS film with a thickness of 135 nm has a average transmittance of 86.26% in the region of 380-1100 nm and reflectance of 54.03% in the rest region of the solar energy spectrum (300-2500 nm). And the ITO SBS film with a thickness of 185 nm has a average transmittance of 78.42% in the region of 380-1100 nm and reflectance of 43.39% in the rest region of the solar energy spectrum. Due to PV solar cells have strong spectrum selection characteristics in the region of 380-1100 nm, we placed the ITO SBS films to PV solar cells for achieving spectrum splitting. The current-

voltage (I-V) and power-voltage (P-V) curve of a PV cell at a total solar irradiance intensity of 1000 W/m² (1 sun) has the shape shown in Fig. 5(b). Moreover, PV cell performance parameters are usually measured by standard test conditions (STC) at a temperature of 25°C and coefficient of air mass (AM) of 1.5. Thereinto, the intersection between the I-V curve and x as well as y axis are open-circuit voltage and short-circuit current, respectively. Based on the I-V curve, we can calculate the power produced by the PV cell via the equation $P=IV$. The I-V curve for a PV cell shows that the current is essentially constant over a range of output voltages, when the total solar irradiance intensity is maintained constant. After adding the ITO SBS film, the short-circuit output current and maximum power of PV cells were decrease due to spectral changes on the surface of the photovoltaic cell. The detailed electrical performance characteristics of original and additional ITO SBS film PV Cells are listed in Tab. 2. The results demonstrate that the original PV cell system achieves the short-circuit current (I_{sc}) of 0.139 A, along with the open-circuit voltage (V_{oc}) of 0.59 V, the maximum Power (P_{MAX}) of 0.058 W, the fill factor (FF) of 0.70, and the photoelectric conversion efficiency (PCE, η) of 14.39%. The PCE was measured by Eq. (4). The ITO SBS film acts as a spectrum splitter, which can transmit the sunlight of wavelength range of 380–1100 nm. The PCE of PV cell were 11.71% and 12.54% when ITO SBS films of 185 nm and 135 nm stack on the PV cells, respectively.

$$\eta = FF \times \frac{I_{sc} \times V_{oc}}{q_{PV} \times A} \times 100\% \quad (\text{eq. 4})$$

where q_{PV} is the solar radiation intensity received on the surface of PV cell, and A is the PV cell area.

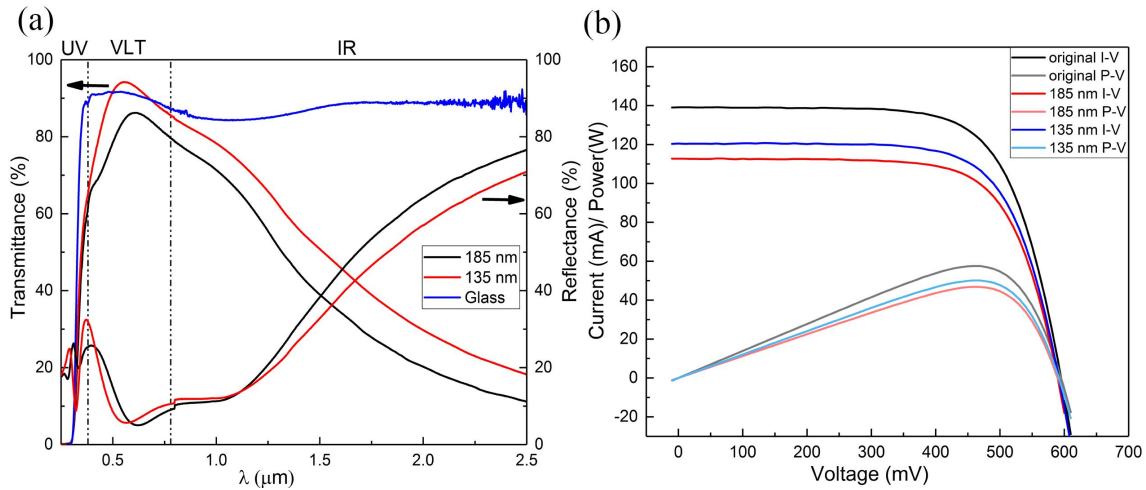


Fig. 5 (a) The transmittance and reflectance spectra of the glass and ITO SBS film, (b) I-V Curve of PV Cell and ITO SBS film

Tab. 2: The electrical performance characteristics of original and additional ITO SBS film PV Cells

	I_{sc} (A)	V_{oc} (V)	P_{MP} (W)	I_{MP} (A)	V_{MP} (V)	FF	η (%)
original	0.139	0.59	0.058	0.125	0.46	0.70	14.39
ITO-185 nm	0.112	0.59	0.047	0.102	0.46	0.71	11.71
ITO-135 nm	0.120	0.59	0.050	0.109	0.46	0.71	12.54

3.2. CPC model

The shape of the CPC varies with the θ_{max} . The larger the CPC θ_{max} , the smaller its maximum opening width and the shorter its reflector plate. That is, the shape of the larger the θ_{max} is more "round" of the CPC. Fig. 6 shows the path light rays diagram increasing the θ_{max} from 20° to 35°.

When the CPC is used in combination with the linear Fresnel reflector system, the light is reflected by the primary reflect mirror cannot all enter the opening of the CPC due to the original CPC reflector blocks a portion of the reflect light. Therefore, part of the CPC reflector blocks needs to be truncated. The ratio of the distance between the CPC opening and the center line of the collector tube and the original reflector plate length of the CPC is called the truncation ratio. The shape of the CPC varies with the truncation ratio, the smaller the length compared to the original CPC reflection plate. Fig. 7 shows the path light rays diagram with different truncation

ratios of CPC. It can be seen that to ensure the uniform distribution of the energy flow density on the absorber tube, the truncation ratio needs to select an appropriate value. Meanwhile, the opening width of CPC is large enough to make all the reflected light of the primary reflect mirror field can enter the CPC and directly reach the surface of the absorber tube. Overall, the proper truncation ratio of the CPC can allow more light into the CPC while greatly reducing the amount of CPC materials and reducing the cost.

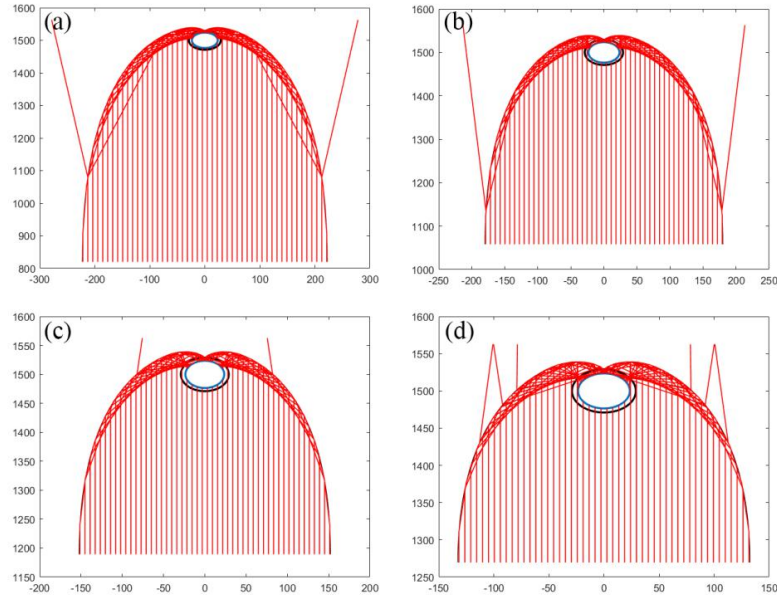


Fig. 6: The path light rays for CPC of different θ_{max} (a)20°, (b)25°, (c)30°, and (d)35°

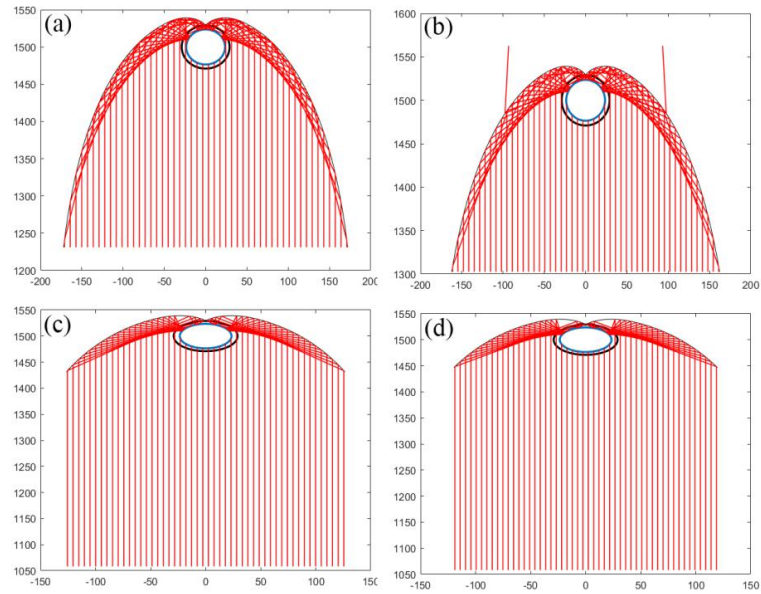


Fig. 7: The path light rays for CPC of different truncation ratios (a)0.9, (b)0.8, (c)0.4, and (d)0.3

3.3. System optical model

Fig. 8 (a) presents the path light rays of the linear Fresnel reflector system, which has a plate at focus position to observe the spot size form the primary reflect mirrors. The analysis of the spots of the primary reflect mirrors found that the light reaches the focus of 1500 mm high with the spot size of about 100 mm, as shown in Fig. 8(b). Therefore, the CPC is designed to ensure that its opening is wide so that all the reflected light has access to the CPC.

After multiple simulation of CPC with different θ_{max} and truncation ratio in Matlab to Tracepro software. The

optimized θ_{max} and truncation ratio of the CPC are 30° and 0.3, respectively. The obtained light path diagram of the linear Fresnel reflector system, as shown in Fig. 9(a). Fig. 9(b) show the map of the circle energy flow density distribution on the surface of the absorber tube with and without ITO SBS filter, which are symmetrical and non-uniformity. As illustrated in this figure, the curvilinear trend of the circle energy flow density distribution with and without ITO SBS filter are significantly consistent; only the values are different. In conclusion, the ITO SBS filters reduce the obtained energy from a single PV system and a single photothermal system.

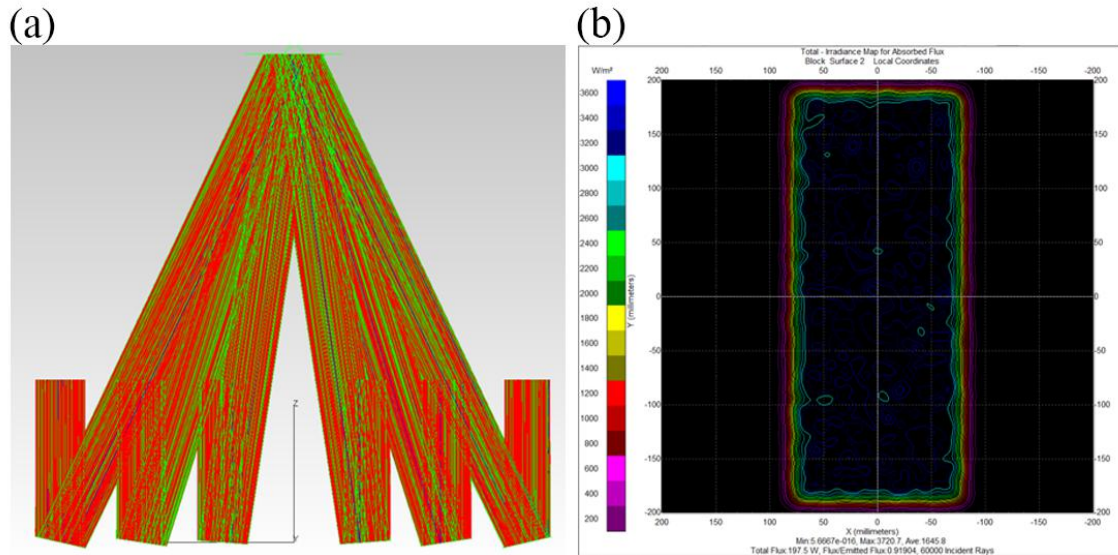


Fig. 8: (a)The path light rays of the linear Fresnel reflector system with a plate, (b) Schematic representation of the spot size of the reflected light at 1500 mm

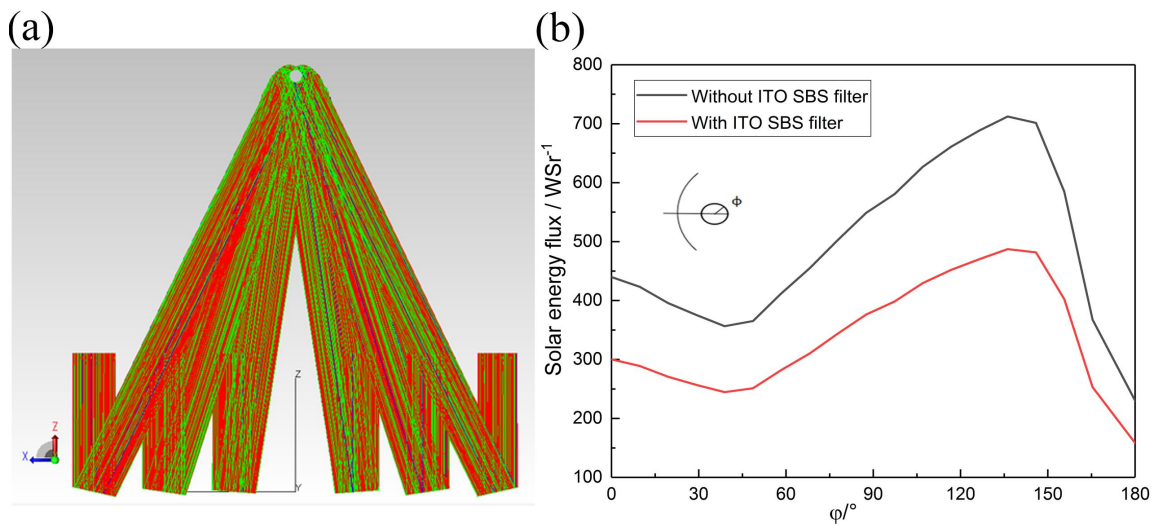


Fig. 9: (a)The path light rays of the linear Fresnel reflector system with a CPC, (b) Solar energy flux distributions on absorber tube

The quantitative analysis finds that the energy calculations are conducted to evaluate the role of the ITO SBS filter of the hybrid PV/CST system. After the addition of the ITO SBS filters, the PV efficiency was reduced by 3.47%, and the photothermal efficiency was decreased by 26.02%. However, the total energy of PV and photothermal using ITO SBS filters was greater than a single PV unit by 33.3%, but decreased by 5.69% compared to individual photothermal units. It could be concluded that adding the ITO SBS filter was promising in hybrid PV/CST system.

4. Conclusion

The PV/CST hybrid system with a novel ITO SBS filter is developed based on the linear Fresnel solar thermal technology. The ITO SBS filter divides the spectrum into two parts, which has high transmittance of 86.26% in

the wavelength range of 300–1100 nm and high reflectance of 54.03% in the wavelength range of 1100–2500 nm. The hybrid PV/CST system utilise the full spectrum sunlight, which exploits transmitted sunlight to PV utilization and reflected sunlight to photothermal utilization, respectively. By using the I-V curve and MCRT method, photoelectric and photothermal characteristics were studied. The photoelectricity conversion efficiency and energy analysys were theoretically calculated. The results indicate that the PCE of PV cell decrease by 12.9% when ITO SBS films of 135 nm stack on the PV cells; the total energy of hybrid PV/CST system using a 135 nm-thick ITO SBS filters was greater than a single PV unit by 33.3%, but decreased by 5.69% compared to individual photothermal units. Moreover, the curvilinear trend of the circle energy flow density distribution with and without ITO SBS filter are significantly consistent. It is concluded that the hybrid PV/CST system with ITO SBS system has enormous potentialities, and it still needs time and vitality to develop in the future.

5. Acknowledgments

This work was funded by the National Key R&D Program of China (No. 2019YFE0102000).

6. References

- Cao, F., Huang, Y., Tang, L., Sun, T. Y., Boriskina Svetlana, V., Chen, G., Ren, Z. F., 2016. Toward a High-Efficient Utilization of Solar Radiation by Quad-Band Solar Spectral Splitting. *Advanced materials*, 28(48).
- Cheng, Z. D., He, Y. L., Cui, F. Q., Xu, R. J., Tao, Y. B., 2012. Numerical simulation of a parabolic trough solar collector with nonuniform solar flux conditions by coupling FVM and MCRT method. *Solar Energy*, 86(6), 1770-1784.
- Felsberger, R., Buchroithner, A., Gerl, B., Schweighofer, B., Wegleiter, H., 2021. Design and testing of concentrated photovoltaic arrays for retrofitting of solar thermal parabolic trough collectors. *Applied Energy*, 300, 117427.
- Han, X. Y., Zhao, X. B., Chen, X. B., 2020. Design and analysis of a concentrating PV/T system with nanofluid based spectral beam splitter and heat pipe cooling. *Renewable Energy*, 162, 55-70.
- Hiba, C., Anissa, G., Jalila, S., Hatem, M., Philippe, B., 2019. A receiver geometrical details effect on a solar parabolic dish collector performance. *Energy Reports*, 5, 882-897.
- Ludman, J. E., Sampson, J. L., Bradbury, R. A., Martin, J. G., Riccobono, J. R., Sliker, G., Rallis, E., 1992. Photovoltaic systems based on spectrally selective holographic concentrators. *Electronic Imaging*, 1667, 182-189.
- Ma, J., Chang, Z., Yan, S. Y., Tian, R., 2017. Energy Flux Distribution and Thermal Performance of Linear Fresnel Collector System in Cold Region. *Energy and Power Engineering*, 9(10), 555-567.
- Qiu, Y., He, Y. L., Cheng, Z. D., Wang, K., 2015. Study on optical and thermal performance of a linear Fresnel solar reflector using molten salt as HTF with MCRT and FVM methods. *Applied Energy*, 146, 162-173.
- Tikhonravov, A. V., Trubetskov, M. K., Debell, G. W., 1996. Application of the needle optimization technique to the design of optical coatings. *Applied Optics*, 35(28), 5493-5508.
- V, P., A, G., 2009. Hybrid photovoltaic_thermal collector based on a luminescent concentrator. *High-efficient low-cost photovoltaics*, 177-181.
- Walzel, M. D., Lipps, F. W., Vanthull, L. L., 1977. A solar flux density calculation for a solar tower concentrator using a two-dimensional hermite function expansion. *Pergamon*, 19(3), 239-253.
- Wang, G., Yao, Y. B., Lin, J. Q., Chen, Z. S., Hu, P., 2020. Design and thermodynamic analysis of a novel solar CPV and thermal combined system utilizing spectral beam splitter. *Renewable Energy*, 155, 1091-1102.
- Widyolar, B., Jiang, L., Winston, R., 2018. Spectral beam splitting in hybrid PV/T parabolic trough systems for power generation. *Applied Energy*, 209(JAN.1), 236-250.
- Zhang, X., Lei, D. Q., Yao, P., Guo, B., Wang, Z. F., 2020. Spectral Beam Splitting Technology for Photovoltaic and Concentrating Solar Thermal Hybrid Systems: A Review. *Journal of Solar Energy Research Updates*, 7, 64-84.
- Zhang, X., Lei, D. Q., Zhang, B., Yao, P., Wang, Z. F., 2021. SiNx/Cu Spectral Beam Splitting Films for Hybrid

Photovoltaic and Concentrating Solar Thermal Systems. ACS omega.

Zhao, D., Xu, E., Yu, Q., Lei, D., 2015. The Simulation Model of Flux Density Distribution on an Absorber Tube. Energy Procedia, 69, 250-258.

Zhou, Y. P., Li, M. J., Hu, Y. H., Ma, T., 2020. Design and experimental investigation of a novel full solar spectrum utilization system. Applied Energy, 260, 114258.